ORIGINAL ARTICLE

Optimization of selective laser melting process parameters for surface quality performance of the fabricated Ti6Al4V

Moses Oyesola[1] · Khumbulani Mpofu[1] · Ntombi Mathe[2] · Samuel Fatoba[3] · Shaik Hoosain[2] · Ilesanmi Daniyan[1]

Abstract
The purpose of this study is to study the influence of the laser power and the scanning speed on the surface hardness, and top surface and side surface roughness of Ti6Al4V metal specimens fabricated via the selective laser melting (SLM) technique. The laser power was varied between 150 and 300 W while the scan speed was varied between 800 and 1400 mm/s. Response surface methodology (RSM) in the Design Expert 11 software environment was used for the design of experiment and results analysis. The distance for surface indentations were targeted at 10–20 μm for the top surface and 60–80 μm for the side surface while the surface hardness profiling was studied using an indenter with the indentation performed at a load of 500 gf and at a dwelling time of 15 s. The study revealed that as the laser power was increased, the surface hardness increases, while the top surface and side surface roughness reduces. Then, when the scanning speed increased, the surface hardness, and top surface and side surface roughness were found to also increase. The optimum range of the process parameters selected are laser speed 300 W and scan speed 1400 mm/s. This produces a minimum surface roughness of 13.006 μm for the top surface roughness and 62.166 μm for the side surface roughness with a corresponding hardness value of 409.391 HV. The findings of this study will assist manufacturers in the process design of the SLM of titanium alloy for aerospace applications.

Keywords SLM · Surface roughness · Surface hardness · Titanium alloy

1 Introduction

The compelling demand to produce quality materials with even surface roughness and excellent mechanical properties for engineering application is part of the practical challenges often encountered during the fabrication of high-strength alloys [1]. Additive manufacturing (AM) is fast gaining industries' attention due to its efficient way of manufacturing and ability to deposit or melt materials in a controlled manner using computer-aided software to create object in a layer-based form during fabrication [2]. Furthermore, AM offers flexibility to conceptualize and fabricate components especially the ones with complex shapes without material wastage and the need for extra machining processes [3–7]. There are a number of advanced techniques in AM especially for end-use production which include fused deposition modeling (FDM), laminated objective manufacturing (LOM), electron beam melting (EBM), laser engineered net shaping (LENS), selective laser sintering (SLS), and selective laser melting (SLM) [8].

SLM is a promising technique of AM technologies and widely adopted for fabricating high-strength alloys such as titanium alloys useful in aerospace applications [9]. This technology uses laser beam to selectively melt metal powder particles together with high accuracy in accordance to the dictate of slices developed by the 3D model. Selective laser melting (SLM) method of additive manufacturing is renowned for production of near-net-shape part, however, with high index of surface roughness. Thus, there is a need to understudy the contributing factors to effective part surface finishing.

Materials developed through this method often retain high relative density in the range that is above 85% and in most

✉ Moses Oyesola
oyesolamo@tut.ac.za

Ntombi Mathe
nmathe@csir.co.za

1 Department of Industrial Engineering, Tshwane University of Technology, Pretoria 0183, South Africa

2 Laser Enabled Manufacturing Unit, National Laser Centre, Council for Scientific and Industrial Research, Pretoria, South Africa

3 College of Aeronautics and Engineering, Kent State University, Kent, OH, USA

cases close to 100% theoretical value [10]. Some of the advantages of using SLM include dimensional accuracy of components developed, fast melting and solidification rates, minimal human interference, and fabrication of materials with high mechanical properties [11]. In spite of the advantages of the SLM process, the rough surfaces accompanying the surface finish of the fabricated component is a limiting factor. This issue hampers the direct industrial applications of the final products from this process unless post-surface finishing operations such as machining is performed [12]. Nonetheless, SLM remains the most unique method for the production of final industrial metal parts where surface roughness is not a major concern [13]. Ti6Al4V powder material among several high-performance alloys has been used in SLM process where the requirements are high strength, lightweight, and potential for heat treatment, and it is often a preferred material for the aerospace, biomedical, and automotive industries [13, 14]. Ti6Al4V alloy combines excellent physical with outstanding mechanical properties; these qualities have placed more demand on the alloy in recent times [14]. Granting the advantages of using SLM for processing metal alloys (Ti6Al4V), the partially melted or un-melted material from the surrounding powder bed sticking to the surface also contributes to its surface roughness [15]. There are factors with significant influence on the smoothness of surface of the component fabricated through SLM method [15]. The crucial parameters are the powder morphology, diameter of the laser beam, layer thickness, scan speed, surface slope angle, and hatch spacing [16–19]. The aforesaid parameters can aid the determination of the morphological properties of material, mechanical, and energy density of SLM developed product. Considering the need to obtain the feasible combination of the process parameters, it is imperative to perform process optimization. This will help in controlling the material and mechanical properties of components in obtaining high surface quality.

Nguyen et al. [20] investigated the influence of powder layer thickness (between 20 and 50 μm) on the SLM printed parts. The authors reported that density and dimensional accuracy of the specimen fabricated increased as the powder layer thickness diminishes. According to Sufiiarov et al. [21], in an investigation conducted on the effect of layer thickness during the fabrication of Inconel 718 superalloy using SLM, higher strength and lower elongation of Inconel 718 could be obtained at 30 μm than at 50 μm layer thickness. Maamoun et al. [22] conducted a study on the influence of SLM process parameters on fabricated Al alloy parts. The authors employed a process map for each material considered in the study by combining the optimized range of SLM process parameters for each characteristic in order to obtain good quality of the as-built parts. This is aimed at improving the dimensional accuracy of the final product and minimizing the need for post-processing. It was observed that optimizing process conditions reduces post-processing operations of the

SLM fabricated Al alloys. Ling et al. [23] studied the optimization of process parameters of SLM technique for manufacturing Ti6Al4V alloy using the RSM. The authors further emphasized the importance of RSM model for designing and processing Ti6Al4V alloy using the SLM technique. This brings to light the essence of optimization of process parameters, especially for the effect of surface error reduction during production and elimination of entire error in approach.

Design of experiment (DoE) approach using response surface methodology (RSM) model has been used by researchers as a design tool to optimize and analyze process parameters uniquely. This is due to its ability to generate feasible combination of input variables, which can be validated via physical experimentations [24–26]. Besides the approach could also generate a mathematical model for correlating the dependent variable (measured response) as a function of the independent variables (process parameters) [24–26]. Qualities such as surface roughness, hardness, dimensional accuracy, density, and mechanical properties of materials have been accurately predicted and investigated with RSM in DoE approach [24–26]. On the other hand, RSM is a collection of statistical and mathematics techniques used for the modeling of processes. The input variables are known as factors that influence the output called responses [27]. The objective of RSM is to establish optimal combination of factors that will produce already optimized response. The use of RSM, its importance, and procedures have been widely reported [28–30]. Lui et al. [31] used RSM approach to investigate the surface morphology of SLM fabricated Ti6Al4V alloy. The optimization of process parameters was analyzed; the focus was on the evaluation of ductility improvement mechanism. The laser power and scanning speed were used as the variable factors while the mechanical properties such as density and material elongation were the responses (output) of the designed experiment. The results obtained indicate that the material elongation increases with the increasing relative density for the fabricated alloy. The authors established the process parameter range that enhances the mechanical properties of the developed Ti6Al4V alloy.

This study developed an experimental model of SLM fabricated Ti6Al4V alloy using the RSM in order to investigate the feasible combination of process parameters that will give optimum surface and hardness responses for Ti6Al4V alloy.

The laser power and scanning speed were the variables selected over a range, based on the existing literature [32–34] for the SLM technique. The attempt made is to correlate the effect of the combined variables on the surface roughness properties of the developed alloy. The fabricated part characteristics were investigated for different SLM parameters to develop a process map that displayed the effect of variables on the part quality. Thus, optimization of SLM process parameters has great benefit in optimizing surface

quality and controlling output of the manufacturing process. The use of titanium alloy for aerospace applications is increasingly emerging [35, 36]; hence, there is still dearth of information regarding the process design using the design of experiment approach validated via physical experimentations for the development of titanium alloy from the SLM technique. The novelty of this work lies in the development of three predictive models for the top surface roughness, side surface roughness, and hardness of titanium alloy fabricated via the SLM technique for two independent process parameters, namely, laser power and scan speed. In addition, the literature have not reported the SLM of titanium alloy at an exact range of 150–300 W for laser power and scan speed varied between 800 and 1400 mm/s. Hence, the findings of this study will assist manufacturers in the process design of the SLM of titanium alloy for aerospace applications. The succeeding sections present the materials and methods, discussion of the findings as well as the conclusion and recommendations.

2 Materials and methods

2.1 Materials

The material used is the composition of gas atomized Ti6Al4V (spherical) with particle average diameter size of 20 μm, Ti grade 5 powder (50 μm), and purity of above 95%. This was supplied by Sigma-Aldrich in South Africa. Table 1 shows the material composition of Ti6Al4V alloy used.

2.2 Experimental equipment and analysis

The manufacturing process involves selective laser melting through powder bed–based additive manufacturing (AM). The manufacturing process permits the development of components with high geometrical complexity to a high degree of surface finish [34]. The experiments were performed using the selective laser machine (Aeroswift platform; CSIR, Pretoria, South Africa). This machine is purposely for metal-additive production using a mix of commercial and locally developed components with capacity to produce part size of $600 \times 600 \times 2000$ mm. In the present study, the optimization of process parameters with a specific range of laser power and scanning speed range was carried out for the developed SLM component. Therefore, block sample size of $10 \times 10 \times 10$ mm^3 was developed by using a constant layer thickness of 50 μm, hatch

spacing of 80 μm, and scanning mode of S-shaped orthogonal with 50% overlap. For the test samples, the orthogonal scanning strategy, which involves the turning of the orientation of the test samples at 90°, was used in this study. The work of Ali et al. [37] already indicates that the scanning strategy of 90° alternating could enhance the hardness, and minimize the residual stresses and subsequently the surface roughness of the test samples when compared to other scanning strategies. Density was not determined on these thin-walled samples due to the fact that they are hollow tube in a thin cube.

The experiment full factor was performed in an optimized setup to obtain proper process parameter combination that includes laser power and scanning speed. The influencing factors or parameters were considered jointly for the fabricated specimen quality analysis. The surface hardness property test complied strictly with ISO 6507-1:2018 [38] on microhardness Vicker tester.

The present study considers the effect of only two process parameters, namely, laser power and scan speed, on the hardness as well as surface and side roughness of the test samples made from titanium powders. The choice of the process parameters stems from their significance in the SLM process as well as their overall influence on the mechanical, microstructure, and surface finish of the final products from the SLM process as indicated by the existing literature [39–50]. Laser power influences the magnitude of the laser energy which in turn influences the rate of melting of the powders and subsequently the mechanical properties and surface finish of the final product. The degree of porosity, density, hardness, uniformity of microstructure, and surface roughness of a product developed from the SLM process is partly a function of the magnitude of the laser power [40–45]. Hence, the laser power is a significant index which reflects the energy absorption rate of the powder during the SLM process. Low magnitude of laser power may result in incomplete melting thus resulting in high porosity, non-uniform microstructure, low density and hardness as well as poor surface finish. On the other hand, when the laser power exceeds the optimum, the process becomes less sustainable in terms of energy consumption and environmental friendliness. It can also cause the product to burn out thereby resulting in surface defect and poor surface finish [44–47].

Scan speed influences the rate of laser energy transfer into the powders during the SLM process. At a low speed, the size of the molten pool may increase although with an increase in the manufacturing cycle time but with the possibility for

Table 1 Powder composition of titanium alloy (Ti6Al4V) [29]

Composition (wt.%)	Al	V	O	H	N	C	Fe	Si	Ti
	5.5–6.75	3.5–4.5	0.15	0.02	0.04	0.04	0.025	0.02	Balanced

Table 2 SLM process preset range for Ti6Al4V as in the literature

Author	Range of process parameters selected	
	Laser power (W)	Scan speed (mm/s)
Sun et al. [42]	380	625–3000
Yakout et al. [43]	40–160	360–1200
Miranda et al. [44]	50–100	417 and 733
Yakout et al.[45]	250	600
Carter et al. [41]	100–200	500–2500
Pal et al. [46]	75	150–1000
Xu et al. [40]	175–375	686–1029
Gong et al. [47]	40–160	360–1200
Shi et al. [48]	400	400–1000
Fogangnolo et al. [49]	171–170	225–1250
Kasperovich et al. [50]	175	200–1100

effective melting and powder consolidation. This may promote a more even spread of the molten pool thereby resulting in the development of products with excellent mechanical properties, uniform microstructure, and surface finish. When the speed exceeds the optimum, the size of the molten pool may decrease which may reduce the flow rate of the molten pool thereby promoting defects such as porosity and surface roughness [45–50].

However, the optimization of these two process parameters will ensure the selection of the feasible range of the process parameters that will influence the development of products with excellent mechanical properties, uniform microstructure, and surface finish in relation to the product's service requirements while ensuring cost and time effectiveness.

The selection ranges have been carefully chosen and determined by considering a similar study on SLM process from which surface roughness within the range of 25–40 μm was

obtained [39]. The selection of the range of the process parameters was also selected based on the works of Xu et al. [40] and Carter et al. [41] after careful review of the existing literature presented in Table 2. Hence, the range selected by the authors is encompassed partially by various studies as presented in Table 2.

The literature have not reported the SLM of titanium alloy at exact selected ranges used in this study. The selected range in this study are within those employed by Xu et al. [40] for laser power and Carter et al. [41] for scan speed selection.

The SLM machine and the test specimen manufactured for this study are shown in Fig. 1a, and b respectively.

The experimental design matrix obtained for two factors levels considered in this study is presented in Table 3. The factor values are in uncoded form for the experiment as conducted in a randomized order to minimize error. As represented in the table, 16 sample experiments were performed for the study analysis. The fitted regression models with the fitness value coefficients are further formulated. The responses are presented in Table 3.

The top and side surface roughness of the samples were measured using the Mitutoyo SJ-201 surface roughness machine.

The surface and side roughness were measured according to EN ISO 4287 and EN ISO 16610-21 standards and the parameters considered during the roughness measurement are presented in Table 4 [51].

2.3 Design of experiment

To reflect on an efficient methodology useful in design of experiment and to reduce the number of unnecessary experiments, a part of a given experimental design, e.g., one fractional factorial design, is often used to generate data. After the operator of a process has gotten used to the equipment, the

Fig. 1 Experimental equipment and manufactured part: **a** the Aeroswift SLM process machine and **b** fabricated part specimen
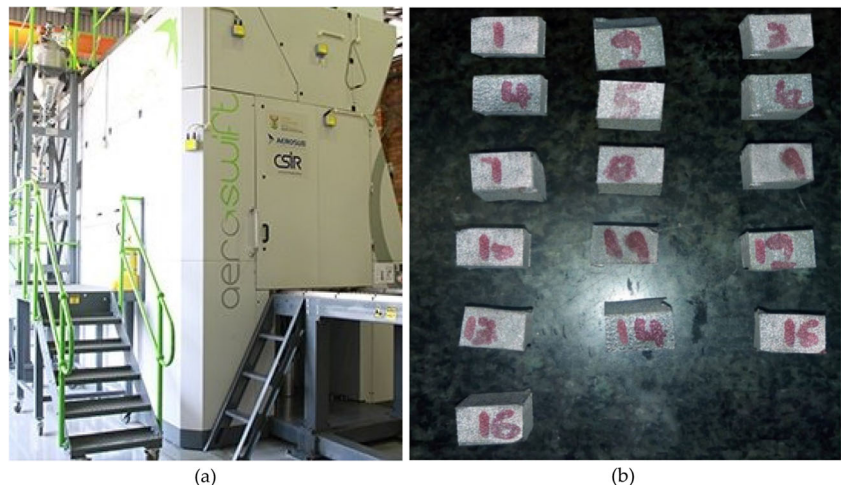
(a)   (b)

Table 3 The selective laser melting (SLM) process parameters used for building the Ti6Al4V alloy and their responses

Runs	Factors		Response 1	Response 2	Response 3
	A: laser power(W)	B: scan speed (mm/s)	Top surface roughness (μm)	Side surface roughness (μm)	Surface hardness (HV)
1	250	800	14.45	71.3	386.6
2	300	1000	13.61	66.3	405.8
3	300	1200	13.52	66.1	406.5
4	250	1000	14.31	71.2	390.9
5	200	1000	15.05	73.7	375.2
6	250	1200	14.07	69.8	393.3
7	200	1200	14.77	72.9	380.7
8	300	1400	12.64	59.7	408.2
9	300	800	13.62	66.5	405.3
10	250	1400	13.73	67.8	401.3
11	150	1000	17.09	86.5	350.2
12	150	1200	16.58	84.9	357
13	150	1400	16.12	79.8	358.5
14	150	800	17.75	87.9	346.1
15	200	1400	14.55	71.9	383.1
16	200	800	15.88	75.9	362.4
Mean			14.86	73.26	381.94
SE			0.36	1.99	5.36
SD			1.44	7.98	21.46
Variance			2.08	63.75	460.48

experimental design can be classified in three parts: screening experiment, response surface model, and verification. Thus, response surface methodology (RSM) method with central composite design (CCD) was used for the SLM process parameter optimization. The general second-order polynomial RSM (full quadratic model) used for the experimental design is expressed as Eq. 1 [52].

$$R_u = \beta_0 + \sum_{i=1}^{n}\beta_i X_{iu} + \sum_{i=1}^{n}\beta_{ii}X_{iu}^2 + \sum_{i<j}^{n}\beta_{ij}X_{iu}X_{ju} + \varepsilon_u, \qquad (1)$$

where R_u is the corresponding response and β_0, β_1, β_{ii}, and β_{ij} represent the regression coefficients. The terms X_{iu} and X_{ju} are

Table 4 Parameters considered for roughness measurement

Parameters	Specification
Dimension of sample (mm³)	10×10×10
Maximum probe tip radius (μm)	2.00
Sampling length (mm)	0.08
Evaluation length (mm)	0.40
Stylus travel (mm)	0.48
Point pitch	Standardized in the measuring device
Cut-off wavelength	Standardized in the measuring device

coded values of the ith and jth input parameters ($i < j$), and ε_u is the residual error. Design Expert version 11 stat-ease software was used for analysis and serves as the regression design and statistical analysis medium for the evaluation of these experimental studies to obtain responses from the influence of the factors.

The RSM has proven to be a suitable approach that can be employed to determine the feasibility of the combination process parameters, their optimum range as well as their cross effects on the response of the designed experiment. It is also a viable tool suitable for process modeling and optimization in order to improve the product's quality as well as the cost and time effectiveness of the manufacturing process [51–54]. With the RSM, the effect of the process parameters (independent variables) on the output target (dependent variables) of the designed experiment can be determined leading to the development of a predictive model for process optimization. As shown in Table 3, the experimental design consists of two factors A and B (A = laser power and B = scan speed) which are the independent variables with three experimental responses (top surface roughness, side surface roughness, and surface hardness) which are the dependent variables. The validation of the numerical experimentation and developed model were validated using ANOVA and the physical experimentations. The indicators of a valid numerical experimentation

Table 5 Study build information

File version	11.1.2.0		
Study type	Response surface	Subtype	Randomized
Design type	Central composite	Runs	16
Design model	Quadratic	Blocks	No blocks
Build time (ms)	2.00		

include F value, adequate precision, "p value Prob > F" which should be less than 0.050, and the correlation coefficients (predicted R^2, R^2, and the adjusted R^2) [55, 56]. The F value is used to examine the statistical significance of the model terms obtained from the individual process parameters or their combination. The larger the F value (>4),the more significant the model terms and vice versa. On the other hand, the p value is a measure of the probability that an observed variation from the statistical mean is a product of random chance. The lower the p value (<0.05), the more significant the model terms and vice versa [55, 56].

3 Results and discussion

The build information for the developed samples is presented in Table 5.

The descriptive statistical analysis of the responses presented in Table 3 was carried out. For the top surface roughness, the SD (1.44) was found to be small, < ± 2, thus indicating that the values of the TSR are close to the mean (14.86). The SE (0.36) and variance (2.08) were also found to be relatively small. This implies that the response data obtained for the top surface roughness are normally distributed. This further implies that the variations in the magnitude of the values of TSR obtained via the physical experimentation are small and that the variations in the magnitude of the process parameters do not have significant influence on the magnitude the top surface roughness, as the experimental values obtained were found to fall within the similar range. For the side surface

roughness, the SD (7.98) was found to be high (> ± 2), thus indicating that the values of the SSR are farther away from the mean (14.86). The SE (1.99) and variance (63.75) were also found to be relatively high. This implies that the response data obtained for the SSR is not normally distributed. This further implies that there exist significant variations in the magnitude of the values of the SSR obtained from the physical experimentations and that the variations in the magnitude process parameters do have significant influence on the magnitude the TSR, as the experimental values obtained differ.

In order to statistically validate the results obtained from the numerical and physical experimentations, ANOVA was carried out and the results obtained are presented in Tables 6, 7, and 8. From Table 4, the high F value (118.35) and small p value (0.0001<0.05) show that the developed model for the TSR is statistically significant and suitable for correlative and predictive purposes. The F value of 118.35 implies the model is significant while there is only a 0.01% chance that an F value this large could occur due to noise. For the TSR model, the R^2 of 0.9834 is in reasonable agreement with the predicted R^2 of 0.9421 and adjusted R^2 of 0.9751 (the differences between the values are less than 0.2) and were found to be close to 1. In addition, the adequate precision with a value 32.914>4 indicates adequate signal-to-noise ratio. The fact that the correlation coefficients were found to be close to unity implies that the developed is statistically significant and suitable for predictive purpose. For the TSR, A, B, and A^2 were the significant model terms (Table 6).

Table 9 presents the three mathematical models for the prediction of the TSR, SSR, and SH (Eqs. 2–7).

Table 6 ANOVA results of the quadratic model for top surface roughness of Ti6Al4V alloys

Source	Sum of squares	df	Mean square	F value	p value	R^2
Top surface	30.73	5	6.15	118.35	< 0.0001	0.9834
A—laser power	26.61	1	26.61	512.47	< 0.0001	
B—scan speed	2.85	1	2.85	54.89	< 0.0001	
AB	0.2016	1	0.2016	3.88	0.0771	
A^2	1.06	1	1.06	20.43	0.0011	
B^2	0.0042	1	0.0042	0.0814	0.7813	
Residual	0.5193	10	0.0519			
Cor total	31.25	15				

Table 7 ANOVA results of the quadratic model for side surface roughness of Ti6Al4V alloys

Source	Sum of squares	df	Mean square	F value	p value	R^2
Side surface	922.66	5	184.53	55.05	< 0.0001	0.9649
A—laser power	817.92	1	817.92	244.00	< 0.0001	
B—scan speed	63.37	1	63.37	18.90	0.0014	
AB	0.7056	1	0.7056	0.2105	0.6562	
A^2	33.64	1	33.64	10.04	0.0100	
B^2	7.02	1	7.02	2.09	0.1784	
Residual	33.52	10	3.35			
Cor total	956.18	15				

Table 8 ANOVA results of the quadratic model for the hardness of Ti6Al4V alloys

Source	Sum of squares	df	Mean square	F value	p value	R^2
Hardness	6823.62	5	1364.72	163.44	< 0.0001	0.9879
A—laser power	6349.27	1	6349.27	760.40	< 0.0001	
B—scan speed	350.70	1	350.70	42.00	< 0.0001	
AB	39.00	1	39.00	4.67	0.0560	
A^2	80.55	1	80.55	9.65	0.0111	
B^2	4.10	1	4.10	0.4911	0.4994	
Residual	83.50	10	8.35			
Cor total	6907.12	15				

3.1 Adequacy of the design for top surface roughness (TSR)

For the TSR model, the fit statistical parameters of the model equation were obtained for the fabricated Ti6Al4V alloys. The predicted R^2 of 0.9421 is in reasonable agreement with the adjusted R^2 of 0.9751 (that is, less than 0.2) and the ratio of 32.914 indicates adequate signal. For the TSR, **A, B, and A^2** were significant model terms and the F value of 118.35 implies the model is significant while there is only a 0.01% chance that an F value this large could occur due to noise. The p values less than 0.0500 as well confirm the significance of the model. Figure 2 presents the normal probability plot of the externally studentized residuals and the predicted versus

actual value response while Fig. 3 presents the top surface roughness in 2D and 3D plot.

From the results obtained, up to 220 W and 1400 mm/s, the magnitude of the laser power and scan speed, respectively, were found to be sufficient, thus, leading to the development of test samples with the targeted surface finish. This was evidenced in the low magnitude of the top surface roughness obtained for the test samples. An increase in the magnitude of the laser power and scan speed were found to be sufficient at 220 W and above 1400 mm/s, respectively. Beyond the value of 220 W, for the laser power, the corresponding surface roughness for the test piece was observed to increase which implies that an increase in the magnitude of the power is no longer desirable

Table 9 Summary of the model equations for the investigated responses

Response	Regression Equations
Top Surface Roughness (TSR)	$TSR = 14.56 - 1.73A - 0.5663B + 0.2021AB + 0.5794A^2 - 0.0366B^2$ (2)
	$TSR = 28.76955 - 0.0792998LP - 0.003014SS + 8.98000E.06LP^*SS + 0.000103^2LP - 4.06250E.07^2 SS$ (3)
Side Surface Roughness (SSR)	$SSR = 72.28 - 9.59A - 2.67B + 0.3780AB + 3.26A^2 - 1.49B^2$ (4)
	$SSR = 124.3255 - 0.407380LP + 0.023757SS + 0.000017LP^*SS + 0.000580LP^2 - 0.000017SS^2$ (5)
Surface Hardness (SH)	$SH = 385.38 + 26.73A + 6.28B - 2.81AB - 5.05A^2 - 1.14B^2$ (6)
	$SS = 190.50850 + 0.897615LP + 0.076884SS - 0.000125LP^*SS - 0.000898LP^2 - 0.000013SS^2$ (7)

Fig. 2 TSR deterministic portion and stochastic error. **a** The normal plot of residuals. **b** The predicted versus actual values (response)
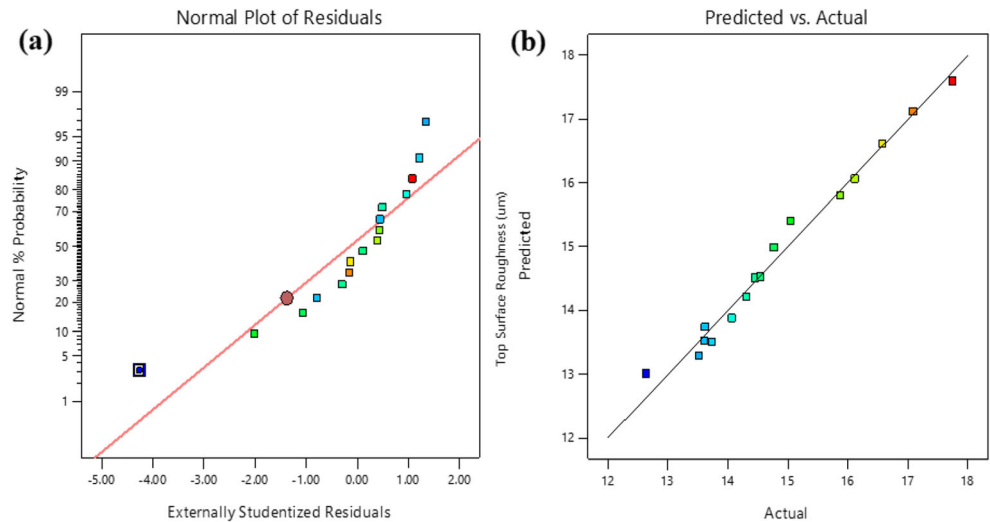
for the process. On the other hand, the laser speed was observed to be desirable at the magnitude beyond 1400 mm/s as evidenced in the reduction of the corresponding surface roughness for the test pieces.

Figure 4 shows the actual (from the physical experimentations) and predicted (from the numerical experimentations) side surface roughness values of Ti6Al4V alloy. From Fig. 2a, the closeness of the data to the average (diagonal) line indicates that the residuals are approximately linear (normal distributed) although with inherent randomness left over within the error portion. In addition, the relationship between the actual and the predicted values of the top surface roughness was found to be significant as indicated by the closeness of the predicted and the actual values represented by the diagonal line. This implies that that the model is adequate for predictive purpose (Fig. 2b). Thus, Fig. 2 presents the experimental plots of residuals as well as the predicted and the actual response values.

The validation of the developed model for the SSR was further carried out via the comparisons of the results obtained from the numerical and physical experimentations. The high degree of agreement between the numerical and physical experimentations as shown by the similarity in the data points shows that the developed model for the prediction of SSR is highly significant (Fig. 4).

3.2 Adequacy of the design for side surface roughness (SSR)

For the **side surface roughness model**, the R^2 of 0.9649 is in reasonable agreement with the predicted R^2 of 0.8920 and the adjusted R^2 of 0.9474 (the differences between the values are less than 0.2) and the adequate precision value of 21.874 >4 indicates adequate signal-to-noise ratio. All the correlation coefficients were found to be close to 1 while **A, B, and A²** were the significant model terms for the SSR. The F value of
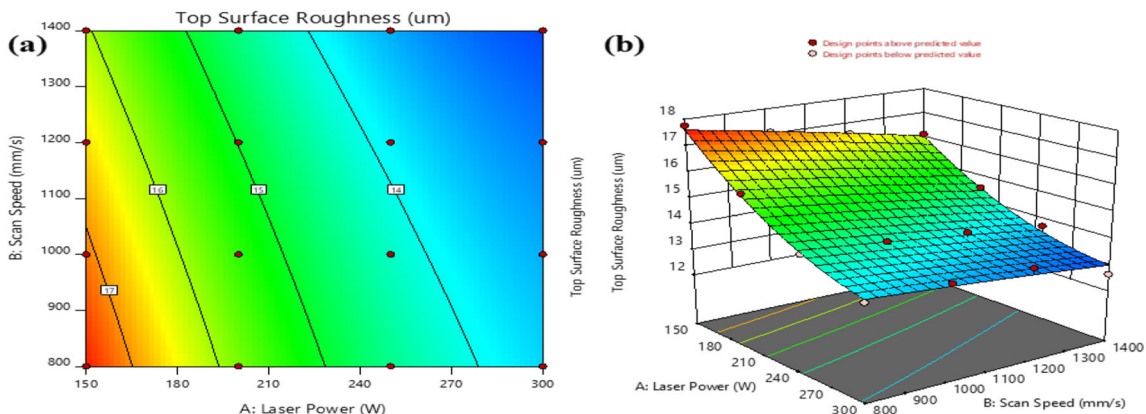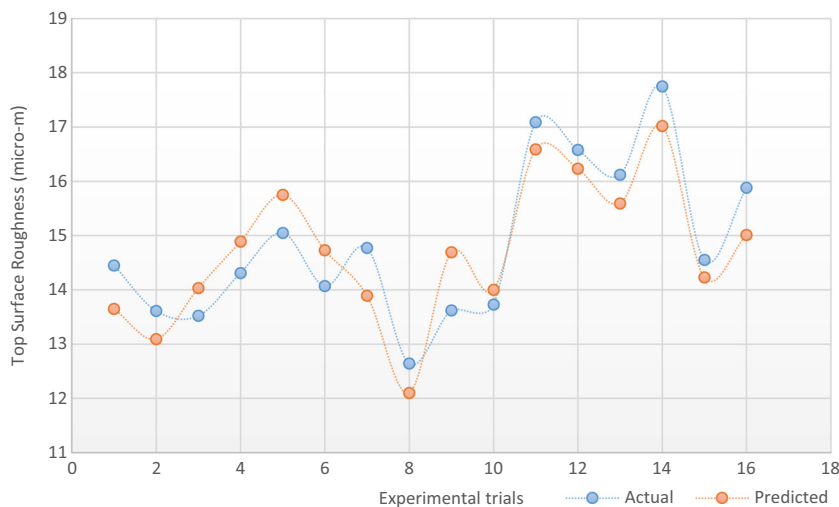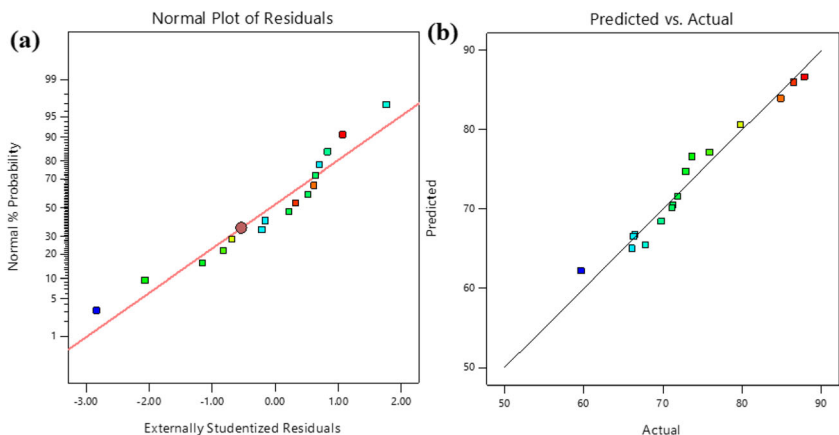

Fig. 3 The 2D and 3D plot of top surface roughness. **a** The contour plot of top surface roughness with respect to scan speed and laser power. **b** 3D RSM plot of top surface roughness with respect to scan speed and laser power

Fig. 4 Actual and predicted side surface roughness values of Ti6Al4V alloy

55.05 implies the model is significant while there is only a 0.01% chance that an F value this large could occur due to noise. The p values less than 0.0500 as well confirm the significance of the model.

Figure 5 presents the normal probability plot of the externally studentized residuals and the predicted versus actual value response.

Figure 6 presents the side surface roughness of 2D and 3D plot of side surface roughness. Figure 7 shows the actual and predicted side surface roughness values of Ti6Al4V alloy.

From Fig. 5a, the closeness of the data to the average (diagonal) line indicates that the residuals are approximately linear (normally distributed) although with inherent randomness left over within the error portion. Obviously, the deviation of the data points from the average line vis-à-vis the average line is permissible. In addition, the relationship between the actual and the predicted values of the side surface roughness was found to be significant as indicated by the closeness of the predicted and the actual values represented

by the diagonal line. This implies that that the model is adequate for predictive purpose (Fig. 5b).

The relationship between the actual and the predicted values of the side surface roughness is shown in Fig. 7. The closeness of the predicted and the actual values as indicated by the similarity in their data pattern indicates that the model is adequate for predictive purpose having inherent randomness left over within the error portion.

3.3 Adequacy of the design for surface hardness (SH)

For the **surface hardness model**, the fit statistical parameters of the model equation were obtained for ANOVA models of Ti6Al4V alloys. The R^2 of 0.9879 is in reasonable agreement with the predicted R^2 of 0.9569 and adjusted R^2 of 0.9819 (the differences between the values are less than 0.2) and the adequate precision value of 37.307 indicates adequate signal-to-noise ratio. For the SH, **A, B, and A^2** were the significant model terms and the F value of 163.44 implies the model is significant while there is only a 0.01% chance that an F value

Fig. 5 Deterministic portion and stochastic error for the side surface roughness of Ti6Al4V alloys. **a** The normal plot of residuals. **b** The predicted versus actual values (response)
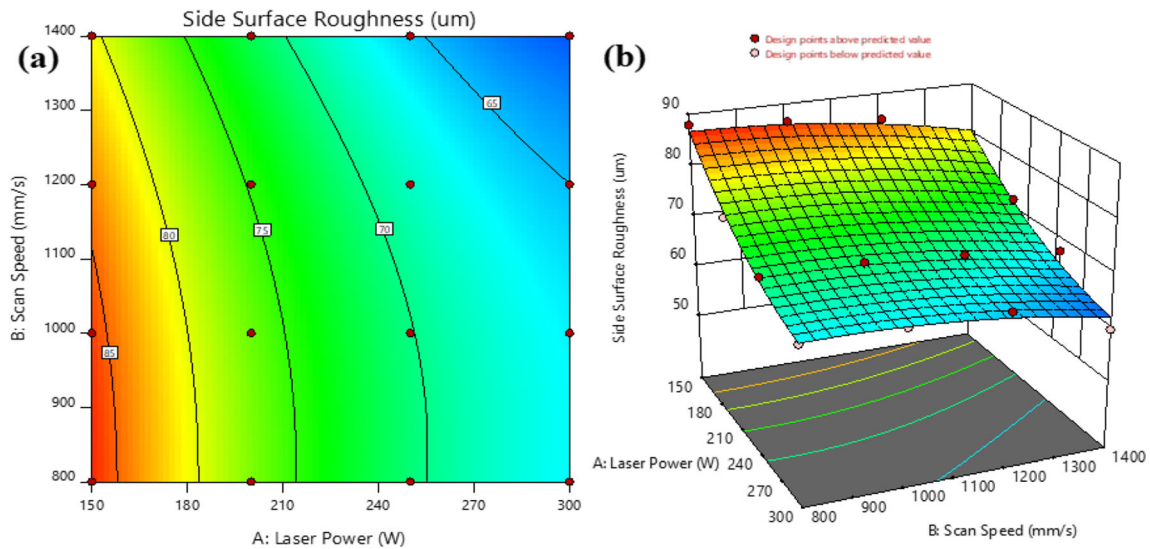
Fig. 6 The 2D and 3D plot of side surface roughness. **a** The contour plot of side surface roughness with respect to scan speed and laser power. **b** 3D RSM plot of side surface roughness with respect to scan speed and laser power

this large could occur due to noise. The *p* values less than 0.0500 as well confirm the significance of the model. Figure 8 presents the normal probability plot of the externally studentized residuals and the coefficient estimate in coded for surface hardness. Figure 9 shows the 2D and 3D plot of side surface roughness.

From the results obtained, up to 270 W and 1300 mm/s, the magnitude of the laser power and scan speed, respectively, were found to be insufficient for the development of the samples to the required surface hardness, thus, leading to the development of test samples with low values of surface hardness. This is because of the input power influences the rate of melting and densification of the powders, which is a function of the material's hardness. An increase in the magnitude of the laser power and scan speed were

found to be sufficient at 300 W and above 1320 mm/s, respectively. Beyond these optimum values, the corresponding surface hardness for the test pieces were observed to increase which imply that an increase in the magnitude of the power and scan speed are no longer desirable for the process. Up to 270 W, the laser power was found to be inadequate to promote rapid plastic deformation of Ti6Al4V with tendency to develop porosity. The higher the porosity, the lower the surface hardness and vice versa. Thus, an increase in the scan speed up to the optimum 1320 mm/s was found to promote the quick interfacial interactions, reflections, and phase transformations with the development of highly densified samples.

Figure 10 shows the experimental relative density versus RSM predicted side surface roughness of Ti6Al4V alloy

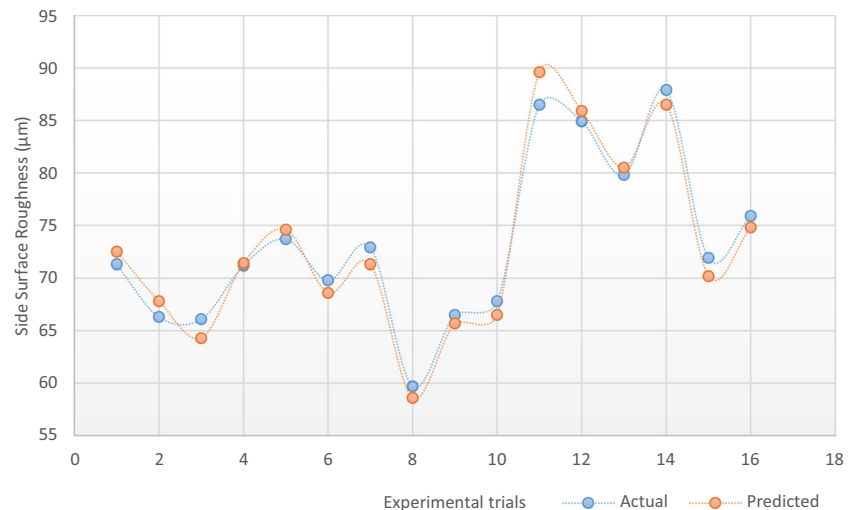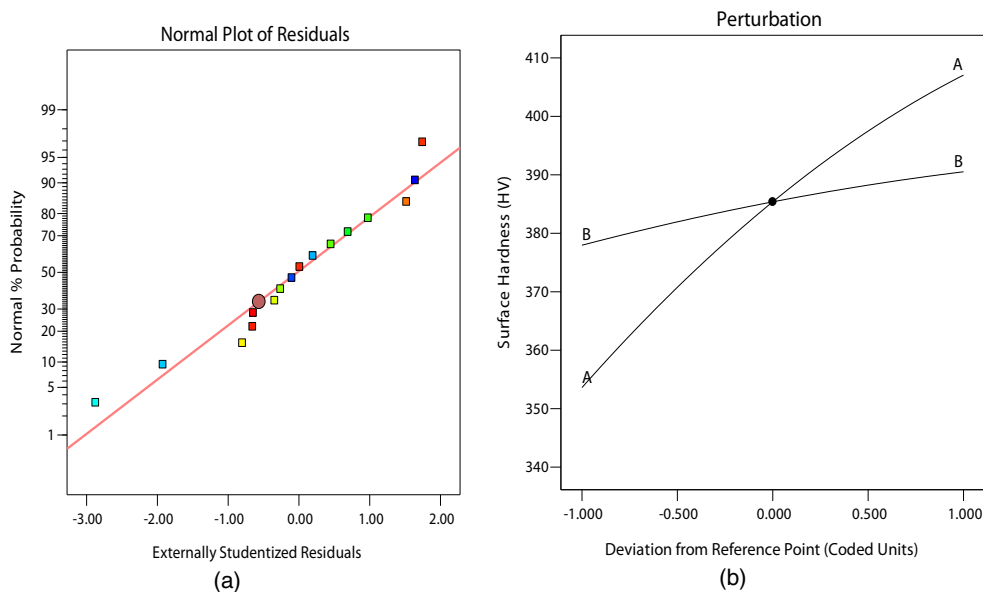**Fig. 7** Actual and predicted side surface roughness values of Ti6Al4V alloy

Fig. 8 **a** The normal probability plot of the externally studentized residuals. **b** The coefficient estimate in coded for surface hardness

(a)

(b)

3.4 Optimized values obtained by the constraints

In the parameter optimisation, nine solutions are found desirable out of the 16 experimental designs. The evaluation data of the optimised parameter sets are presented in Table 10 for the productivity and surface quality values. For the range of the optimized process parameters, the magnitude of the top surface roughness ranges from a minium value of 13.006 to 13.303 μm while the side surface roughness ranges from a minimum value of 62.166 μm to a maximum value of 62.516 μm. The magnitude of the surface hardness ranges

from a minimum value of 407.742 HV to a maximum value of 409.391 HV. Hence, the optimum magnitude of the process parameters selected are laser speed 300 W and scan speed 1400 mm/s. This produces a minimum surface roughness of 13.006 μm for the top surface roughness, and 62.166 μm for the side surface roughness with a corresponding hardness value of 409.391 HV.

The optimal process parameters for both surfaces' laser power (LP = 300 W) and scanning speed (SS = 1400 mm/s) which gave a minimum top surface roughness and side roughness of 13.006 μm and 62.166 μm, respectively, at surface
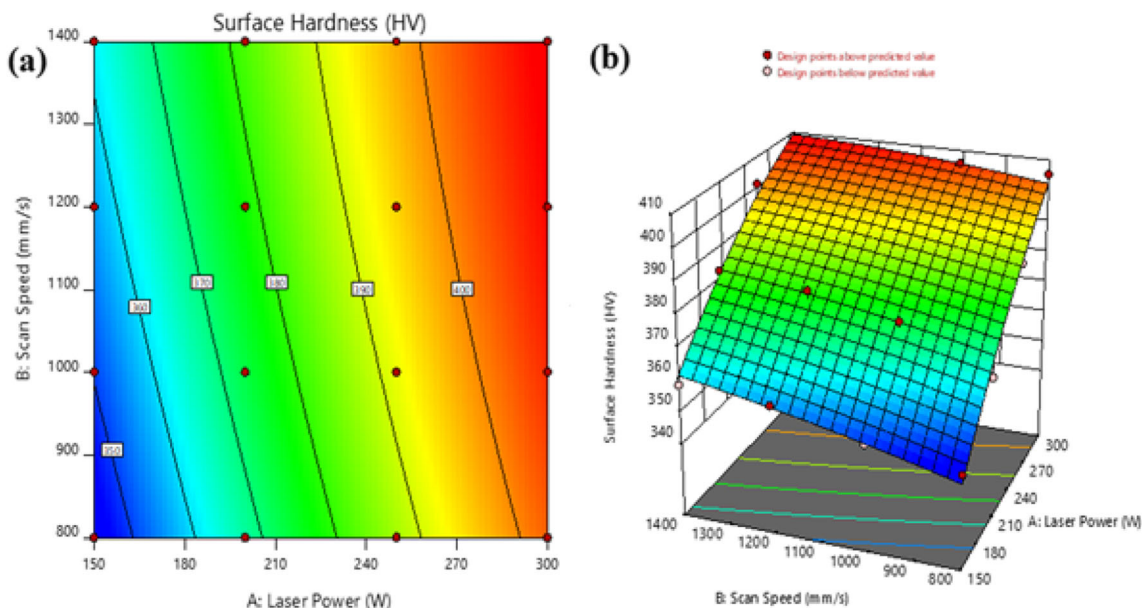

Fig. 9 The 2D and 3D plot of top surface hardness. **a** The contour plot of surface hardness with respect to scan speed and laser power. **b** 3D RSM plot of surface hardness with respect to scan speed and laser power

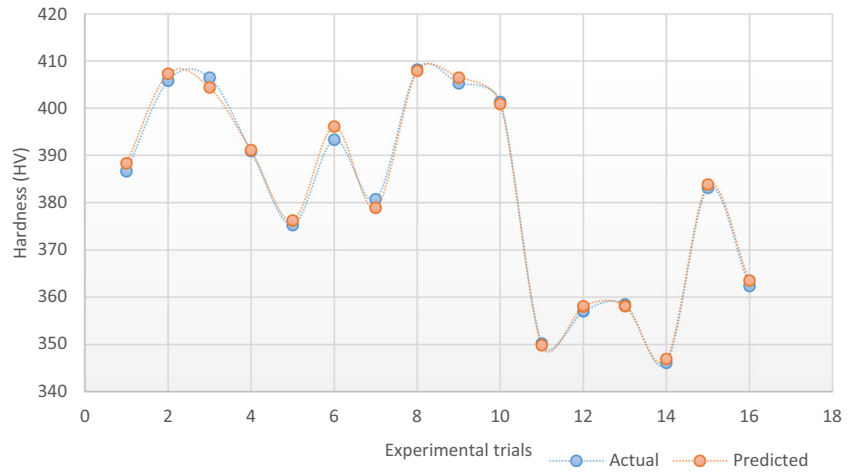**Fig. 10** Actual and predicted side surface hardness values of Ti6Al4V alloy

Table 10 Optimised values obtained and default parameters

Number	Laser power (W)	Scan speed (mm/s)	Top surface roughness (μm)	Side surface roughness (μm)	Surface hardness (HV)	Desirability	
1	300.000	1400.000	13.006	62.166	409.391	0.946	Selected
2	298.967	1399.997	13.011	62.203	409.200	0.945	
3	297.310	1399.997	13.020	62.266	408.889	0.944	
4	296.593	1399.999	13.024	62.294	408.753	0.943	
5	294.734	1400.000	13.034	62.370	408.396	0.942	
6	293.337	1399.997	13.043	62.430	408.123	0.940	
7	291.408	1399.997	13.055	62.516	407.742	0.936	
8	299.999	1319.285	13.121	63.476	408.987	0.922	
9	300.000	1182.879	13.303	65.201	407.931	0.887	

hardness 409.391 produced a desirability value of 0.946. The practitioners in industry can choose the best parameter set from this table based on their needs, considering the balance between surface quality and productivity of different industrial components. Figure 11 represents the main effect plot for the influencing parameters.

Fig. 11 The main effect plot for the parameters
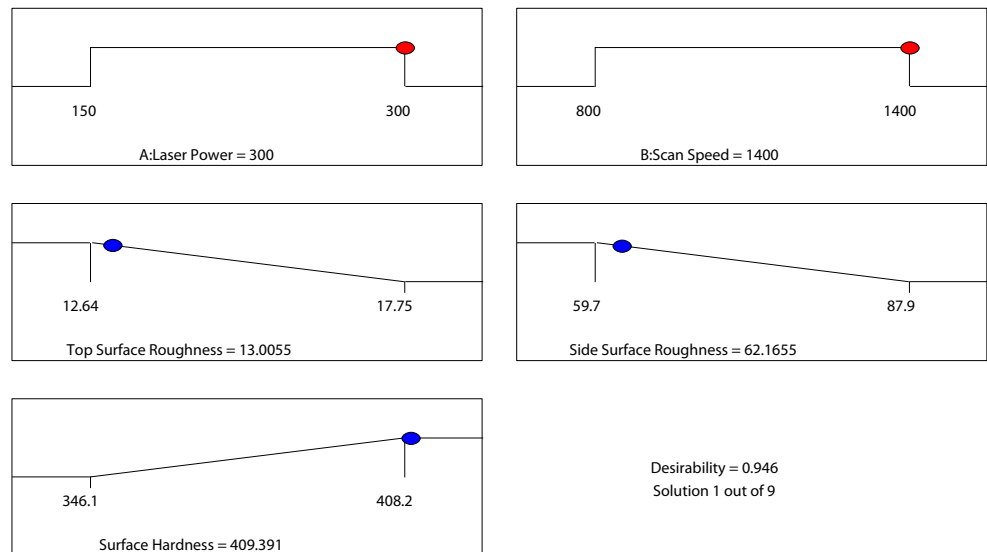
4 Conclusions

The purpose of this study was to study the influence of the laser power and the scanning speed on the surface hardness, and top surface and side surface roughness of Ti6Al4V metal specimens fabricated via the selective laser melting (SLM) technique. This was achieved using the design of experiment technique involving the use of the response surface methodology validated via physical experimentations.

The experimental results show that quality with respect to roughness and hardness of the fabricated component part is affected by laser power and scanning speed as far as minimizing roughness is concerned. The statistical analyses of the results obtained show the significance of the predcitive models for the top surface roughness, side surface roughness, and hardness of the fabricated Ti6Al4V samples. The results show that the coefficient of determination (R^2) for the developed model indicates the developed regression model fits for the actual data. This study shows that there is a need for a right combination of processing parameters to attain the targeted required values within a given micron range. The study indicated that TSR, SSR, and SH can be optimized concurrently to obtain better response. The optimum magnitude of the process parameters selected were laser speed 300 W and scan speed 1400 mm/s. This produces a minimum surface roughness of 13.006 μm for the top surface roughness and 62.166 μm for the side surface roughness with a corresponding hardness value of 409.391 HV.

From the three response surfaces, the three output parameters show a monotonic relationship with the two input parameters (LP and SS), for example, the top surface roughness can be further reduced by either increasing SS or LP. In view of this, future works can consider the extension of the range of the process parameters for improved optimization in order to get the peak of the process parameters that will promote optimum hardness and minimum surface roughness. Furthermore, this study considers the orthogonal scanning strategy, other exposure parameters such as contour exposure, and upskin and downskin parameters can be considered as part of the future study. In addition, process conditions such as the exposure time, point distance, contouring method as well as the upskin and downskin parameters can also be considered.

The effect of the hatching distance on the mechanical properties of the metal parts produced using the SLM process as well as the effect of the processing conditions on residual stresses of titanium alloy are also recommended.

Declarations

Conflict of interest The authors declare that they have no conflict of interest.

References

1. Strano G, Hao L, Everson RM, Evans KE (2013) Surface roughness analysis, modelling and prediction in selective laser melting. J Mater Process Technol 213(4):589–597
2. International, A. (2010) ASTM F2792-09e1 standard terminology for additive manufacturing technologies. ASTM International, Pennsylvania. [Google Scholar]
3. DebRoy T, Wei HL, Zuback JS, Muckherjee T, Elmer JW, Milewski JO, Beese AM, Wilson-Heid A, De A, Zhang W (2017) Additive manufacturing of metallic components–process, structure and properties. Prog Mater Sci 92:112–224
4. Oyesola MO, Mpofu K, Mathe NR, Daniyan IA (2019) Development of an integrated design methodology model for quality and throughput of additive manufacturing processes. Procedia CIRP 84:688–693
5. Daniyan IA, Mpofu K, Daniyan OL, Fameso F, Oyesola M (2020) Computer aided simulation and performance evaluation of additive manufacturing technology for component parts manufacturing. Int J Adv Manuf Technol 107:4517–4530
6. Oyesola MO, Mpofu K, Mathe NR, Daniyan IA (2020) Hybrid-additive manufacturing cost model: a sustainable through-life engineering support model for maintenance repair overhaul in the aerospace. Procedia Manuf 49:199–205
7. Daniyan IA, Balogun V, Mpofu K, Omigbodun FT (2020) An interactive approach towards the development of an additive manufacturing technology for railcar manufacturing. Int J Interact Des Manuf 14:651–666
8. Gong H, Rafi K, Gu H, Starr T, Stucker B (2014) Analysis of defect generation in Ti–6Al–4V parts made using powder bed fusion additive manufacturing processes. Addit Manuf 1:87–98
9. Oyesola M, Mathe N, Mpofu K, Fatoba S (2018) Sustainability of additive manufacturing for the South African aerospace industry: a business model for laser technology production, commercialization and market prospects. Procedia CIRP 72:1530–1535
10. Aliakbari M (2012) Additive manufacturing: state-of-the-art, capabilities, and sample applications with cost analysis. School of Industrial Engineering and Management, KTH Royal Institute of Technology, Stockholm
11. Schmidt M, Merklein M, Bourell D, Dimitrov D, Hausotte T, Wegener K, Overmeyer L, Vollertsen F, Levy GN (2017) Laser based additive manufacturing in industry and academia. CIRP Ann 66(2):561–583

12. Kumar LJ, Nair CGK (2017) Current trends of additive manufacturing in the aerospace industry. Springer Science + Business Media, Singapore. In: Wimpenny DI, Pandey PM, Kumar LJ (eds) Advances in 3D printing & additive manufacturing technologies. Springer, pp 39–54

13. Najmon JC, Raeisi S, Tovar A (2019) Review of additive manufacturing technologies and applications in the aerospace industry. In: Froes F, Boyer R (eds) Additive manufacturing for the aerospace industry. Elsevier, pp 7–31

14. Xu W, Lui EW, Pateras A, Qian M, Brandt M (2017) In situ tailoring microstructure in additively manufactured Ti-6Al-4V for superior mechanical performance. Acta Mater 125:390–400

15. Rehme O, Emmelmann C (2005) Reproducibility for properties of selective laser melting products. In: Proceedings of the Third International WLT-Conference on Lasers in Manufacturing, Munich

16. Taguchi G, Chowdhury S, Taguchi S (2000) Robust engineering. McGraw-Hill, New York

17. Badkar DS, Pandey KS, Buvanashekaran G (2011) Parameter optimization of laser transformation hardening by using Taguchi method and utility concept. Int J Adv Manuf Technol 52(9-12): 1067–1077

18. Shipley H, McDonnell D, Culleton M, Lupoi R, O'Donnell G, Trimble D (2018) Optimisation of process parameters to address fundamental challenges during selective laser melting of Ti-6Al-4V: a review. Int J Mach Tools Manuf 128:1–20

19. Li Z, Kucukkoc I, Zhang DZ, Liu F (2018) Optimising the process parameters of selective laser melting for the fabrication of Ti6Al4V alloy. Rapid Prototyp J 24(1):150–159

20. Nguyen QB, Luu DN, Nai SML, Zhu Z, Chen Z, Wei J (2018) The role of powder layer thickness on the quality of SLM printed parts. Arch Civ Mech Eng 18(3):948–955

21. Sufiiarov VS, Popovich AA, Borisov EV, Polozov IA, Masaylo DV, Orlov AV (2017) The effect of layer thickness at selective laser melting. Procedia Eng 174:126–134

22. Maamoun AH, Xue YF, Elbestawi MA, Veldhius SC (2018) Effect of selective laser melting process parameters on the quality of Al alloy parts: powder characterization, density, surface roughness, and dimensional accuracy. Materials 11(12):2343

23. Ling TY, Kumar JR (2017) Design, optimization and characterization of azilsartan nanoparticles using Design-Expert® software version 11. Rapid Prototyp J 3:395–407

24. Ituarte IF, Coatanea E, Salmi M, Tuomi J, Partanen J (2015) Additive manufacturing in production: a study case applying technical requirements. Phys Procedia 78:357–366

25. Daniyan IA, Mpofu K, Adeodu AO (2019) Optimization of welding parameters using Taguchi and response surface methodology for rail car bracket assembly. Int J Adv Manuf Technol 100: 2221–2228

26. Tlhabadira IA, Daniyan IA, Masu L, Mpofu K (2020) Computer aided modelling and experimental validation for effective milling operation of titanium alloy (Ti6AlV). Procedia CIRP 91:113–120

27. Yap CY, Chua CK, Dong ZL, Zhang DQ, Loh LE, Sing SL (2015) Review of selective laser melting: materials and applications. Appl Phys Rev 2(4):041101

28. Ribeiro F, Sergio LM, Lauro CH, Bueno AHS, Brandao LC (2016) Influence cutting parameters on the surface quality and corrosion behavior of Ti–6Al–4V alloy in synthetic body environment (SBF) using Response Surface Method. Measurement 88:223–237

29. Boschetto A, Bottini L, Veniali F (2018) Surface roughness and radiusing of Ti6Al4V selective laser melting-manufactured parts conditioned by barrel finishing. Int J Adv Manuf Technol 94(5-8):2773–2790

30. Jou YT, Lin WT, Lee WC, Yeh TM (2014) Integrating the Taguchi method and response surface methodology for process parameter optimization of the injection molding. Appl Math Inf Sci 8(3): 1277–1285

31. Liu R, Wang Z, Liou F, Newkirk J (2017) Aerospace applications of laser additive manufacturing. In: Brandt M (ed) Laser additive manufacturing: materials, design, technologies, and applications. Woodhead Publishing Series in Electronic and Optical Materials, pp 351–371

32. Poprawe R, Hinke C, Meiners W, Schrage J, Bremen S, Merkt S (2015) SLM production systems: recent developments in process development, machine concepts and component design. In: Brecher C (ed) Advances in production technology. Lecture Notes in Production Engineering, pp 49–65

33. Gebhardt A, Hötter J-S, Ziebura D (2014) Impact of SLM build parameters on the surface quality. RTejournal-Forum für Rapid Technologie 2014(1):1–13

34. Tshabalala LC, Mathe N, Chikwanda H (2018) Characterization of gas atomized Ti-6Al-4V powders for additive manufacturing. Key Eng Mater 770:3–8

35. Daniyan IA, Tlhabadira I, Mpofu K, Adeodu AO (2020) Development of numerical models for the prediction of temperature and surface roughness during the machining operation of titanium alloy (Ti6Al4V). Acta Polytechnica J 60(5):369–390

36. Daniyan IA, Tlhabadira I, Phokobye SN, Mrausi S, Mpofu K, Masu L (2020) Modelling and optimization of the cutting parameters for the milling operation of titanium alloy (Ti6Al4V). 2020 IEEE 11th International Conference on Mechanical and Intelligent Manufacturing Technologies (ICMIMT 2020). Added to IEEE Xplore, pp 68-73

37. Ali H, Ghadbeigi H, Mumtaz K (2018) Effect of scanning strategies on residual stresses and mechanical properties of selective laser melted Ti4Al4V. Mater Sci Eng A 712:175–187

38. Park H, Tran N, Nguyen D (2017) Development of a predictive system for SLM product quality. In: IOP Conference Series: Materials Science and Engineering. IOP Publishing

39. Sun J, Yang Y, Wang D (2013) Parametric optimization of selective laser melting for forming Ti6Al4V samples by Taguchi method. Opt Laser Technol 49:118–124

40. Xu W, Brandt M, Sun S, Elambasseril J, Liu Q, Latham K, Xia K, Qian M (2015) Additive manufacturing of strong and ductile Ti–6Al–4V by selective laser melting via in situ martensite decomposition. Acta Mater 85:74–84

41. Carter LN, Essa K, Attallah MM (2015) Optimisation of selective laser melting for a high temperature Ni-superalloy. Rapid Prototyp J 21(4):423–432

42. Sun Z, Tan X, Tor SB, Yeong WY (2016) Selective laser melting of stainless steel 316L with low porosity and high build rates. Mater Des 104:197–204

43. Yakout M, Elbestawi MA, Veldhuis SC (2020) A study of the relationship between thermal expansion and residual stresses in selective laser melting of Ti-6Al-4V. J Manuf Process 52:181–192

44. Miranda G, Faria S, Bartolomeu F, Pinto E, Madeira S, Mateus A, Carreira P, Alves N, Silva FS, Carvalho O (2016) Predictive models for physical and mechanical properties of 316L stainless steel produced by selective laser melting. Mater Sci Eng A 657:43–56

45. Yakout M, Elbestawi MA, Veldhuis SC, Nangle-Smith S Influence of thermal properties on residual stresses in SLM of aerospace alloys. Rapid Prototyp J 26(1):213–222

46. Pal S, Lojen G, Kokol V, Drstvensek I (2018) Evolution of metallurgical properties of Ti6Al-4V alloy fabricated in different energy densities in the selective laser melting technique. J Manuf Process 35:538–546

47. Gong H, Rafi H, Starr T, Stucker B (2013) The effects of processing parameters on defect regularity in Ti-6Al-4V parts fabricated by selective laser melting and electron beam melting. 24th Annual International Solid Freeform Fabrication Symposium, University of Texas, p 424–39

48. Shi X, Ma S, Liu C, Wu Q, Chen X, Lu J (2016) Performance of high layer thickness in selective laser melting of Ti6Al4V. Materials 9(12):975

49. Fogagnolo J, Sallica-Leva E, Najar Lopes ES, Jardini A, Caram R (2012) The effect of the laser process parameters in the microstructure and mechanical properties of Ti6Al4V produced by selective laser sintering/melting. 21st International Conference on Metallurgy and Materials (Metal 2012), p 1234–8

50. Kasperovich G, Haubrich J, Gussone J, Requena G (2016) Correlation between porosity and processing parameters in TiAl6V4 produced by selective laser melting. Mater Des 105: 160–170

51. Mitutuyo Quick guide to surface roughness measurement. Bulletin no 2229, 2016. [Online] Available at https://www.mitutoyo.com/wp-content/uploads/2012/11/1984_Surf_Roughness_PG.pdf. Accessed 11 Mar 2021

52. Baligidad SM, Chandrasekhar U, Elangovan K, Shankar S (2018) RSM optimization of parameters influencing mechanical properties in selective inhibition sintering. Mater Today: Proc 5(2):4903–4910

53. Daniyan IA, Mpofu K, Oyesola MO, Daniyan L (2020) Process optimization of additive manufacturing technology: a case evaluation of a manufactured railcar accessory. Procedia CIRP 95:89–96

54. Daramola OO, Tlhabadira I, Olajide JL, Daniyan IA, Sadiku ER, Masu L (2019) Process design for optimal minimization of resultant cutting force during the machining of Ti-6Al-4V: response surface method and desirability function analysis. Procedia CIRP 84:854–860

55. Daniyan IA, Tlhabadira I, Phokobye SN, Siviwe M, Mpofu K (2019) Modelling and optimization of the cutting forces during Ti6Al4V milling process using the response surface methodology and dynamometer. MM Sci J 128:3353–3363

56. Daniyan IA, Fameso F, Ale F, Bello K, Tlhabadira I (2020) Modelling, simulation and experimental validation of the milling operation of titanium alloy (Ti6Al4V). Int J Adv Manuf Technol 109(7):1853–1866